The effect of membrane tension on specific adhesion in steady-state between soft elastic materials

Xinyao Zhu*[a, b], Wangjiang Lin[a], Yanling Tian [a, b]

[a] Key Laboratory of Mechanism Theory and Equipment Design of Ministry of Education, Tianjin University, Tianjin 300350, China

[b] School of Engineering, University of Warwick, Coventry CV4 7AL, UK

Keywords: specific adhesion; molecular bond; receptor-ligand; optimal adhesion; membrane tension; surface tension

Abstract

This present study investigates the effect of membrane tension on the molecular-mediated adhesion between two soft elastic materials in a steady state, which simulates the specific adhesion between two cells with cyto-membrane tension taken into consideration. A coupled surface elasticity-bulk elasticity-stochastic model is developed to describe the adhesive contact scenario, which is represented by a Fredholm's equation of the second kind. The numerical results show that the rupture behavior of the two elastic materials transmits from Griffith-like mode to Bell's model when the adhesion size decreases. Unlike the classic case (Wang and Gao, 2010), the pull-off stress exhibits a non-monotonic dependence on the adhesion size ascribed to the presence of membrane tension. In addition, the interfacial stresses become evenly distributed attributed to membrane tension, which again verifies the conclusion that membrane tension facilitates adhesion optimization.

1. Introduction

It is well-known that surface adhesion plays a significant role in the contact mechanics of micro/nano scales. In this area, the JKR theory (Johnson et al., 1971) predicts well the adhesive contact behavior of large and compliant spheres, whereas the DMT (Derjaguin et al., 1975) theory is appropriate for small and stiff spheres. The transition between DMT and JKR models is realized by the Maugis-Dugdale model (Maugis, 1992), where the Dugdale cohesive zone model is utilized to characterize the interfacial stresses. Later on, Greenwood (1997) adopted the Lennard-Jones potential law to simulate the interaction forces, and also presented the JKR and DMT extremes, in terms of pull-off forces.

Contrary to the above studies where the adhesion is due to nonspecific interactions such as van der Waals forces, substantial attention has been paid to adhesive contacts mediated by specific molecular bonds (Evans, 1985a, b; Qian et al., 2008; Qian et al., 2009; Wang and Gao, 2010; Qian et al., 2013; Qian et al., 2017), namely known as receptor-ligand bonds (Alberts et al., 2002). It is known that molecular bonds are responsible for the interaction between cells and extracellular matrices and play a paramount role in many adhesion-mediated cellular processes, such as migration, spreading, differentiation, growth and healing, known as mechanotransduction, even though the molecular bonds were subsequently integrated into the context of standard peel test (Evans 1985 a, b; Dembo et al., 1988; Freund and Lin, 2004). For example, Evans (1985 a, b) developed a peeling model for membrane-membrane adhesion which is mediated by continuous specific molecular bonds, whereas the prototype of this model is presumably the contact between two cells with cyto-

membrane tension. In the present study, membrane tension is considered to be responsible for the separation between two adherent membranes, which enables us to investigate how membrane tension affects specific adhesion.

Here we use on the conception of surface tension to simulate membrane-membrane tension[1] in cell interactions. The surface tension stems from surface effect that atoms (or molecules) on the surface of materials behave differently from those within the bulk. The surface effect is related to the ratio of surface tension to the elastic modulus of the bulk material, which is considered as an intrinsic material length. To elucidate the surface effect, Gurtin and Murdoch (1975, 1998) developed a 3D theory based on continuum mechanics. The Gurtin-Murdoch (G-M) surface elasticity predicts well the results from experiments and atomic simulations (Miller and Shenoy, 2000; Shenoy, 2002), in terms of some elementary deformation modes. In this regard, this theory prevails in the explanation of many size dependent phenomena at nanoscale (Altenbach et al., 2012; He et al., 2004; Huang, 2008; Lu et al., 2011). Following the G-M surface elastic theory, Hajii (1978) obtained the Green's function of an elastic half-space with constant surface tension, based on which Hajii et al. (1979) improved the measurements of shear modulus and pleural membrane tension of the lung. Inspired by Hajii's work, the present study aims to investigate the effect of cyto-membrane tension on the specific adhesion by means of the concept of surface effect, whose prototype is the molecular bonds-mediated adhesion between two cells with cyto-membrane tension taken into account. On the other hand, previous studies which successfully characterize the effect of surface tension on nonspecific adhesion (Hui et al., 20015; Zhu and Xu, 2018) would provide substantial support for the present study, in terms of computational methods.

2. Theoretical background

The G-M surface elasticity theory assumes that the surface of a material is a thin membrane of negligible thickness which ideally adheres to the bulk. Reminiscent of the fact that ctyo-membrane thickness (7-8 nanometers) is infinitesimal compared to the size of cells (usually several microns), the G-M surface theory would be a plausible characterization for cytoplasm and cyto-membrane (with constant tension) system. In another word, the cytoplasm and cyto-membrane are modeled as an elastic half-space and a film of infinitesimal thickness respectively. The bulk material (cytoplasm) has the same equilibrium and constitutive equations as those of the classical elasticity theory.

The equilibrium equations of the membrane are written as (Chen et al., 2006; Mogilevskaya et al., 2011)

$$\sigma^{s}_{\alpha\beta,\beta} = \sigma_{ij} n_i \nu^{\alpha}_{j} - t_{\alpha} \quad (1)$$

$$\sigma^{s}_{\alpha\beta,\beta} \kappa_{\alpha\beta} = \sigma_{ij} n_i n_j - t_3 \quad (2)$$

where $\sigma^{s}_{\alpha\beta}$ is the membrane stress tensor, σ_{ij} is the bulk stress tensor, $\mathbf{n}(n_1, n_2, n_3)$ is the unit normal vector to the membrane, $\boldsymbol{\nu}^{\alpha}(\nu^{\alpha}_1, \nu^{\alpha}_2, \nu^{\alpha}_3)$ is the unit tangential vector along the x_α direction, $\mathbf{t}(t_1, t_2, t_3)$ is the membrane traction, and $\kappa_{\alpha\beta}$ is the curvature tensor of the deformed membrane. For repeated Greek indices (1, 2) and Latin indices (1, 2, 3), Einstein's summation convention is adopted. For the membrane with constant tension, the membrane stress can be simply given as

$$\sigma^{s}_{\alpha\beta} = \tau^{0} \delta_{\alpha\beta} \quad (3)$$

In this sense, Hajii (1978) developed the Green's function where the bulk material is regarded as an infinite elastic half-space:

[1] The present study does not distinguish membrane tension from cyto-membrane tension deliberately.

$$\sigma_z(r,0) = \frac{P}{2\pi s}\{\frac{\pi}{2s}[H_0\left(\frac{r}{s}\right) - Y_0\left(\frac{r}{s}\right)] - \frac{1}{r}\} \quad (4)$$

$$u(r,0) = -\frac{(1-2\nu)P}{4\pi G}\int_0^\infty \frac{J_1(rt)}{1+st}dt \quad (5)$$

$$w(r,0) = \frac{P}{4\Gamma}[\ H_0\left(\frac{r}{s}\right) - Y_0\left(\frac{r}{s}\right)\ ] \quad (6)$$

where $s = \tau^0(1 - \nu)/G$ is an intrinsic material length indexing the relative significance of surface tension. The shear modulus and Poisson's ratio are denoted by G and ν respectively. $H_n(\cdot)$, $J_n(\cdot)$ and $Y_n(\cdot)$ denote the Struve function, Bessel function of the first kind and Bessel function of the second kind, respectively, and n is the order. P is a concentrated normal force.

3. The model

To illustrate the scenario of the contact problem stated above, Fig. 1 depicts the axisymmetric contact problem of two elastic half-spaces connected by a cluster of ligand-receptor bonds which constitute an adhesion patch whose radius is a. The two half-spaces are covered with membrane of infinitesimal thickness with constant tension as mentioned above.

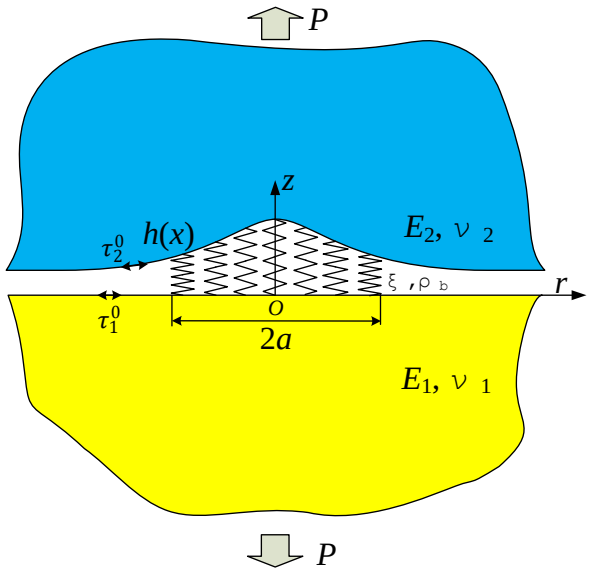

Fig. 1. Schematic illustration of molecular bonds-mediated adhesion between two elastic materials with membrane tension.

Throughout this study, we only consider specific adhesion due to ligand-receptor linkages, and ignore secondary nonspecific interactions, e.g. van der Waals forces. The cylindrical coordinate (r, φ, z) is adopted as shown in Fig. 1, where the origin is located at the center of the adhesion patch of the lower substrate, so that the upper and lower surfaces are located at $z = h(x)$ and $z = 0$ respectively, where $h(x)$ denotes shape function. It is hypothesized that in the adhesion patch area, there are ρ_t pairs of ligand-receptor bonds per unit area, of which ρ_b bonds are closed.

The surface displacement w_1 and w_2, corresponding to the lower and upper elastic half-spaces respectively, can be formulated in terms of the normal traction $p(x)$ between the two surfaces as (Zhu and Xu 2018)

$$w_1(r) = -\frac{1}{2\tau_1^0}\int_{t=0}^{a} p(t)tdt \int_{\theta=0}^{\pi}[H_0\left(\frac{\sqrt{r^2+t^2-2rt\cos\theta}}{s_1}\right) - Y_0(\frac{\sqrt{r^2+t^2-2rt\cos\theta}}{s_1})]\,d\theta \quad (7)$$

$$w_2(r) = \frac{1}{2\tau_2^0}\int_{t=0}^{a} p(t)tdt \int_{\theta=0}^{\pi}[H_0\left(\frac{\sqrt{r^2+t^2-2rt\cos\theta}}{s_2}\right) - Y_0(\frac{\sqrt{r^2+t^2-2rt\cos\theta}}{s_2})]\,d\theta \quad (8)$$

where τ^0_i (hereafter i = 1, 2) denotes the membrane tension of the two materials, and $s_i = \tau^0_i(1 - \nu_i)/G_i$. The relative displacement $w(r)$ between the two surfaces is given as

$$w(r) = w_1(r) - w_2(r) \quad (9)$$

According to the geometrical relation, one has

$$e(r) + w(r) = h(r) \quad (10)$$

where $e(r)$ denotes the elongation. Here we consider a simple shape $h(r) = a\kappa[1 - (r/a)^2]$. For simplicity, the closed bonds are treated as Hookean springs with stiffness ξ, and thus one has

$$p(r) = -\xi\rho_b(r)w(r) \quad (11)$$

The reversible transitions between rebinding and dissociation of the ligand-receptor bonds are assumed to be governed by a chemical reaction (Orsello et al., 2001):

$$[R] + [L] \Leftrightarrow [B] \quad (12)$$

where $[R]$, $[L]$ and $[B]$ represent the densities of the receptors, the ligands and the receptor-ligand bonds respectively. In this regard, the ligand-receptor bond density is ruled by a simple kinetic relationship (Wang et al., 2008):

$$\frac{d\rho_b(r,\tau)}{d\tau} = \gamma[\rho_t(r,\tau) - \rho_b(r,\tau)] - e^{\xi u/F_b}\rho_b(r,\tau) \quad (13)$$

In the steady state ($\tau\to\infty$), one has

$$\rho_b(r) = \frac{\gamma\rho_0}{\gamma + exp[\frac{\xi w(r)}{F_b}]} \quad (14)$$

Inserting Eqs. (7), (8), (11) and (14) into Eq. (10) results in

$$e(t) + \sum_{i=1}^{2}\frac{1}{2\gamma_i}\int_{t=0}^{a} G\left(\frac{r}{s_i},\frac{t}{s_i}\right) t\,\xi\frac{\gamma\rho_0}{\gamma+\exp\left[\frac{\xi e(t)}{F_b}\right]}e(t)dt = a\kappa[1-\left(\frac{r}{a}\right)^2] \quad (15)$$

Introducing the following dimensionless parameters:

$$\rho = \frac{\rho_b}{\rho_0}, \tau = \frac{t}{a}, \varrho = \frac{r}{a}, \quad \alpha_i = \frac{\xi a\rho_0}{E_i^*}, \beta_i = \frac{E_i^*}{\rho_0 F_b}, s_i' = \frac{s_i}{a}, e' = \frac{\xi}{F_b}e, Q = \frac{P}{a\rho_0 F_b} \quad (16)$$

Eq. (15) is rewritten as

$$e'(\varrho) + \sum_{i=1}^{2}\frac{\alpha_i}{s_i'}\int_{\tau=0}^{1} G\left(\frac{\varrho}{s_i'},\frac{\tau}{s_i'}\right)\frac{\gamma e'(\tau)}{\gamma+exp[e'(\tau)]}\tau d\tau = \alpha_1\beta_1\kappa(1-\varrho^2) \quad (17)$$

It is noted that Eq. (17) is the Fredholm's equation of the second kind, and Newton-Raphson iteration method is adopted to solve this equation.

4. Results and discussions

Eq. (17) denotes a coupled elastic-membrane tension-stochastic model, which enables us to investigate the validation of the concept of Griffith and Bell molecular adhesion in the presence of membrane tension. By assuming the two half-spaces have the same mechanical properties[2] and after solving the Fredholm's equation of the second kind given in Eq. (17), the relationship between the normalized pull-off stress and normalized cluster size under different normalized membrane tension values is illustrated in Fig. 2.

[2] In this regard, one has $\alpha_1 = \alpha_2 = \alpha$, $\beta_1 = \beta_2 = \beta$ and $s'_1 = s'_2 = s'$ according to Eq. (16).

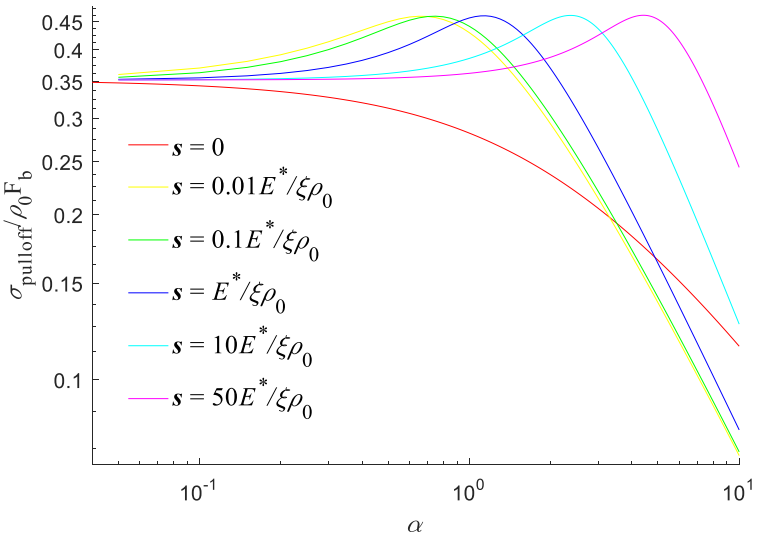

Fig.2. Dependence of normalized pull-off stress on adhesion size, under $\gamma = 2$, $\kappa = 0$ and $\beta = 5$.

Following Bell (1978), when the bond density reaches the steady state without any external load, the strength of molecular adhesion (σ_{Bell}) is given as

$$\sigma_{Bell} \propto \frac{\gamma\rho_0}{1+\gamma}\xi u_{max} = \frac{\gamma\rho_0}{1+\gamma}\xi\frac{F_b}{\xi} = \frac{\gamma\rho_0 F_b}{1+\gamma} \quad (18)$$

In this sense, Eq. (18) can be rewritten as

$$\frac{\sigma_{Bell}}{\rho_0 F_b} = C_B\frac{\gamma}{1+\gamma} \quad (19)$$

As shown in Fig. 2, for a single α-$\sigma_{\mathrm{off}}/\rho_0 F_{\mathrm{b}}$ curve, as the cluster size approaches zero, the normalized pull-off stresses converge to approximately 0.35, irrespective of the value of $s\xi\rho_0/E^*$, which coincides with Eq. (19) because infinitesimal cluster size corresponds to zero external load. On the other hand, as the adhesion size increases largely enough, there exhibits a linear relation between the normalized pull-off stress and normalized adhesion size in the logarithmic coordinate, which resembles the classic situation, i.e. the Griffith concept where the normalized pull-off stress is inversely proportional to the square root of the normalized adhesion size (Wang and Gao, 2010). In general, Fig. 2 presents the transition of adhesion behavior between Griffith's theory and Bell's molecular adhesion theory, even if with the presence of membrane tension.

For a certain value of s, as the adhesion size increases, the normalized pull-off stress rises from 0.35 to the maximum value (approx. 0.46) and dramatically decays. Compared with the classic situation (c.f. the red curve in Fig. 2), there is a non-monotonic dependence of the normalized pull-off stress on the normalized adhesion size when surface tension is taken into consideration. Moreover, the normalized adhesion size corresponding to maximum pull-off stress decreases as the surface tension weakens[3], and thus one can predict that the pull-off stress decreases monotonically with α increasing when surface tension is zero (i.e. the red curve in Fig. 2). Alternatively speaking, the peak point in the $\sigma_{\mathrm{pulloff}}$–$\alpha$ curves shifts in lower left direction as surface tension weakens, and thus one can predict that this vertex would land on the ordinate as surface tension is null, which is the red curve in Fig. 2.

[3] In fact, the maximum pull-off stress decreases moderately as the surface tension decreases by a careful comparison.

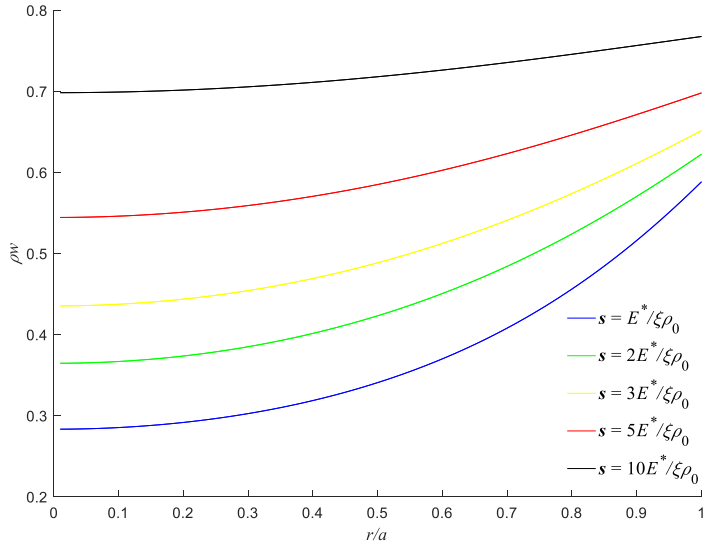

Fig.3. Radial distribution of interfacial stress corresponding to $\gamma = 5$, $\kappa = 0$, $\beta = 5$ and $\alpha = 2$

Gao and Yao (2004) have indicated that the optimal adhesion between a flat-ended cylinder and a substrate could be realized by size reduction if the adhesion is non-specific, and this conclusion is also confirmed for adhesion via molecular bonds by Wang and Gao (2010). However, for the latter situation, when membrane tension is taken into account, it is observed that the normalized pull-off stress becomes saturated faster with membrane tension enhanced, as adhesion size decreases, which indicates that membrane tension tends to enhance the behavior of optimal adhesion. In addition, with other parameters fixed, a stronger membrane tension would result in a more uniform distribution of interfacial stresses, as shown in Fig. 3, which again demonstrates that membrane tension would facilitate optimal adhesion. Furthermore, the non-monotonic relation between pull-off stress and adhesion size implies that the existence of membrane tension would incur a maximum pull-off stress, which would potentially facilitate optimal adhesion.

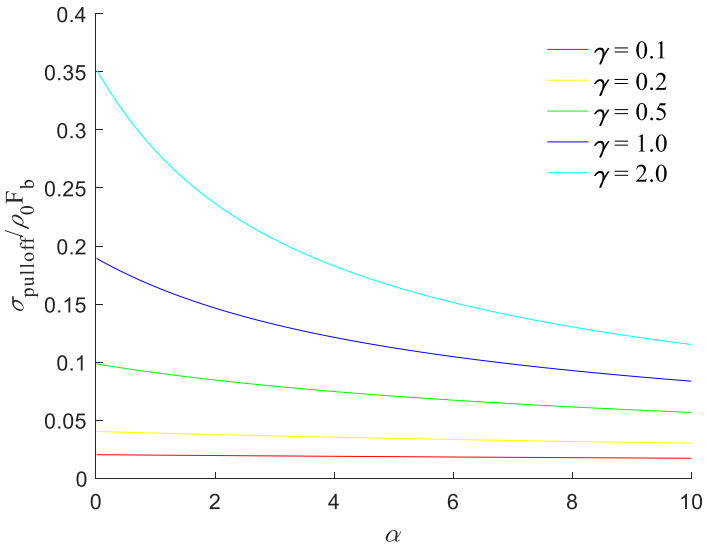

(*a*)

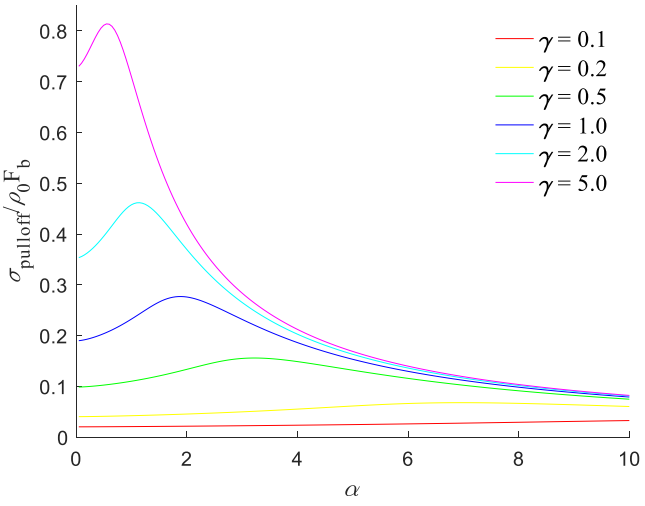

(*b*)

Fig.4. The dependence of pull-off stress on normalized adhesion size α under different binding rates, where $\kappa = 0$, $\beta = 5$, for (*a*) $s = 0$ (classic case) and (*b*) $s = E^*/\xi\rho_0$,

Fig. 4 illustrates the dependence of normalized pull-off stress on the parameter α, where the dimensionless rebinding rate γ varies with other parameters fixed. It can be seen that, for a given α, higher rebinding rate results greater pull-off stress, which is consistent with one's intuition. Contrary to the non-surface tension situation [Fig. 4(*a*)], the relationship between α and normalized pull-off stress is non-monotonic in the membrane tension case as illustrated in Fig. 4(*b*). The peak point in the curve keeps move in up-left direction as the rebinding rate γ strengthens. Therefore, it is revealed that the presence of membrane tension affects the impact of rebinding rate (γ) on the pull-off stress.

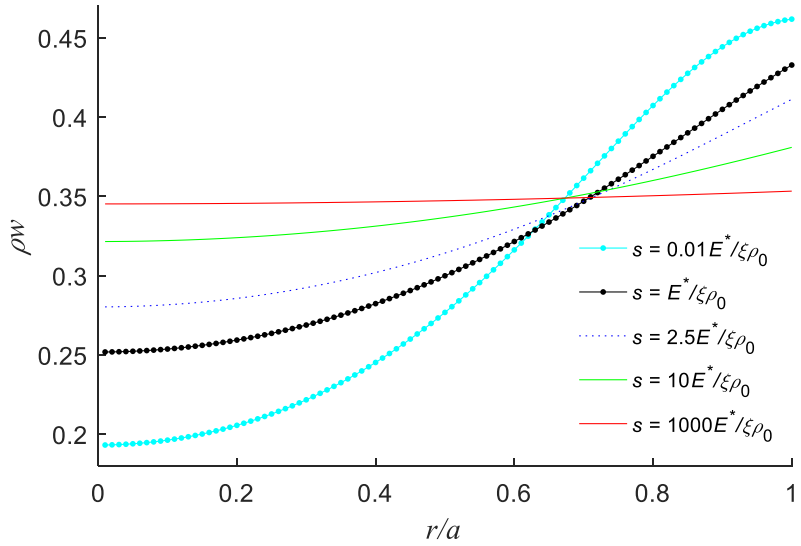

Fig.5. Radial distribution of interfacial stress under $\alpha = 1$, $\gamma = 2$, $\kappa = 0.1$ and $Q = 0.17$.

Fig. 5 shows the effect of surface tension on the distribution of interfacial stress. With other parameters fixed, it is observed that increasing surface tension would cause a more even distribution of the stress. As the surface tension decreases, the interfacial traction distribution tends to be singular, with minimum and maximum stress being at the center and edge respectively. Noticing that the stress concentration index[4] $\alpha = 10$ is relatively high, Fig. 5 indicated that increasing surface tension can weaken the stress singularity on the edge.

Fig. 6 shows the distribution of normalized density of closed bonds under different membrane tensions. It can be seen that the density of closed bonds tends to be evenly distributed as membrane tension increases. For a small membrane tension, the density of closed bonds is evenly distributed in the center and drops dramatically at the edge. Reminding that the parameter ρ denotes the ratio of closed ligand-receptor bonds, which play a significant role in the transfer of mechanical stimuli in mechanotransduction of cells. In this sense, one can predicts that membrane tension can ultimately regulate mechanotransduction behavior of cells.

[4] The adhesion size α can also be regarded as stress concentrated index, as defined by Qian et al. (2008)

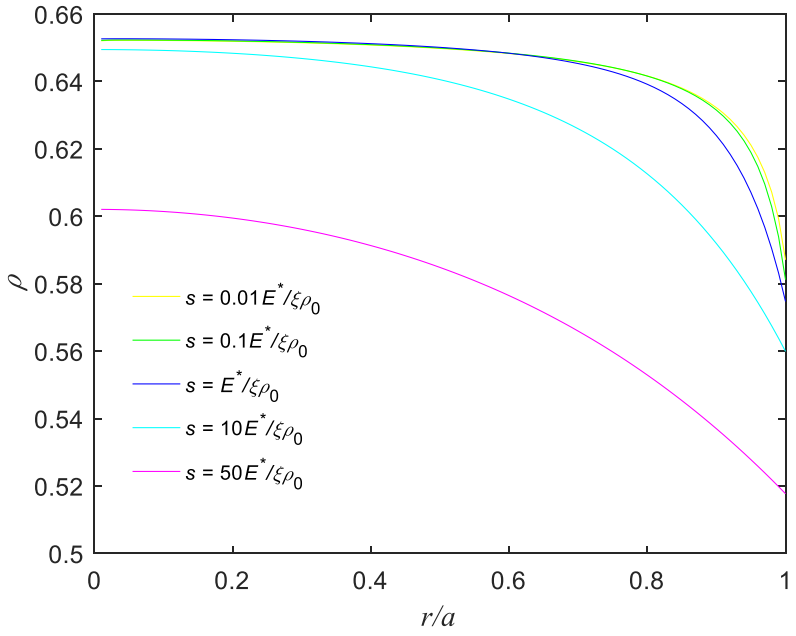

Fig.6. Radial distribution of the normalized density of closed bonds, with $\alpha = 10$, $\gamma = 2$, $\kappa = 0$ and $\beta = 5$.

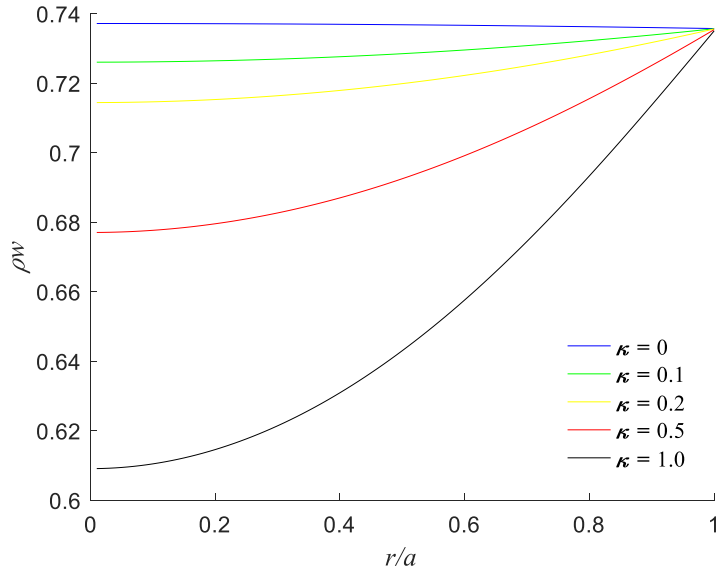

(*a*)

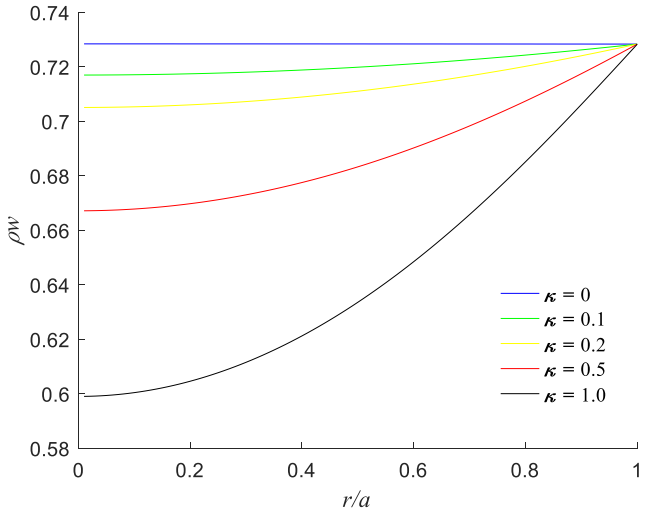

(*b*)

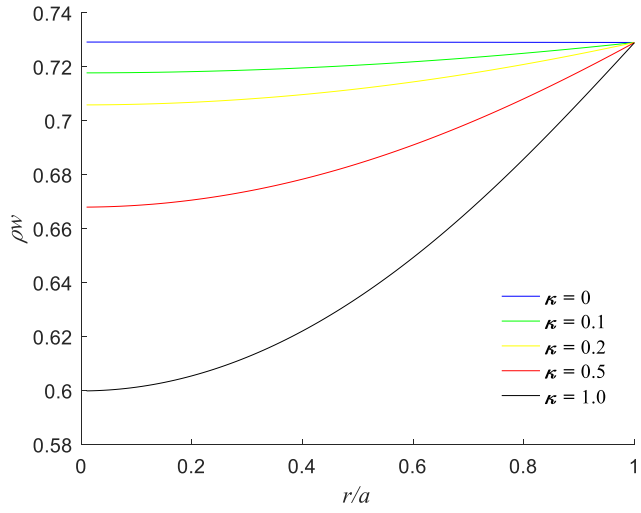

(*c*)

Fig. 7. Radial distribution of interfacial stresses corresponding to different rebinding rates, under $\alpha = 0.1$, $\beta = 5$ for (*a*) $s = E^*/\xi\rho_0$, (*b*) $s = 10E^*/\xi\rho_0$ and (*c*) $s = 20E^*/\xi\rho_0$

Fig. 7 shows the distribution of interfacial stress for different contact profiles represented by κ = 0, 0.1, 0.2, 0.5 and 1.0. It can be seen that the stress concentration at the adhesion edge increases as κ increases, which is opposite to the situation in non-surface tension. This indicates the membrane tension can inversely alter the dependence of stress concentration on the parameter κ. On the other hand, when the surface tension increases, the bandwidth of the interfacial stress corresponding to κ = 0, 0.1, 0.2, 0.5 and 1.0 decays, indicating that it becomes less insensitive to variations of the contact surface profile.

5. Conclusions

The present study combines continuum mechanics, surface elasticity theory and stochastic mechanics concepts to study how cyto-membrane tension affects specific adhesion mediated by molecular bonds, which is represented by a Fredholm's equation of the second kind. The numeric

results indicate that the pull-off behavior exhibits a transition from Griffith like mode by crack propagation at the edge to the Bell type of even bond rupture, as the adhesion size keeps decreasing. However, the pull-off stress presents a non-monotonic dependence on the adhesion size due to the existence of cyto-membrane tension, implying that manipulation of cyto-membrane tension can contribute to the optimal adhesion. This conclusion is further verified by the fact that interfacial stresses are evenly distributed sue to surface tension. The results presented in this study would shed potential light on the effect of cyto-membrane tension on mechanotranduction of biological cells.

Conflicts of interest

There are no conflicts in the present study.

Acknowledgements

The author is very grateful for the financial supports from the China-EU H2020 International Science and Technology Cooperation Project (2017YFE0112100) and H2020-MSCA-RISE Project (FabSurfWAR-644971).

References

Alberts, B., Johnson, A., Lewis, J., Raff, M., Roberts, K., Walter, P., 2002. Molecular Biology of the Cell, fourth ed. Garland Science, New York.

Altenbach, H., Eremeyev, V.A., Morozov, N.F., 2012. Surface viscoelasticity and effective properties of thin-walled structures at the nanoscale. Int. J. Eng. Sci. 59, 83–89.

Bell, G.I., 1978. Models for the specific adhesion of cells to cells. Science, 200, 618–627.

Chen, T.Y., Chiu, M.S., Weng, C.N., 2006. Derivation of the generalized Young–Laplace equation of curved interfaces in nanoscaled solids. J. Appl. Phys. 100, 074308.

Derjaguin, B.V., Muller, V.M., Toporov, Y.P., 1975. Effect of contact deformations on the adhesion of particles. J. Coll. Interface Sci. 53, 314–326.

Dembo, M., Torney, D.C., Saxman, K., Hammer, D., 1988. The reaction-limited kinetics of membrane-to-surface adhesion and detachment. In: Proceedings of the Royal Society Series B-Biological Sciences, vol. 234, pp. 55–83.

Evans, E.A., 1985a. Detailed mechanics of membrane-membrane adhesion and separation. 1. Continuum of molecular cross-bridges. Biophys. J. 48, 175–183.

Evans, E.A., 1985b. Detailed mechanics of membrane-membrane adhesion and separation. 2. Discrete kinetically trapped molecular cross-bridges. Biophys. J. 48, 185–192.

Freund, L.B., Lin, Y., 2004. The role of binder mobility in spontaneous adhesive contact and implications for cell adhesion. J. Mech. Phys. Solids 52, 2455–2472.

Gao, H., Yao, H., 2004. Shape insensitive optimal adhesion of nanoscale fibrillar structures. Proc. Natl. Acad. Sci. U. S. A 101, 7851–7856.

Greenwood, J.A., 1997. Adhesion of elastic spheres. Proc. R. Soc. Lond. A 453, 1277–1297.

Gurtin, M.E., Murdoch, A.I., 1975. A continuum theory of elastic material surfaces. Arch. Ration. Mech. Anal. 57, 291–323.

Gurtin, M.E., Weissmuller, J., Larché, F., 1998. A general theory of curved deformable interfaces in solids at equilibrium. Philos. Mag. A 78, 1093–1109.

Hajji, M.A., 1978. Indentation of a membrane on an elastic half space. J. Appl. Mech. 45, 320–324.

Hajii, M.A., Wilson, T.A., Lai-Fook, S.J., 1979. Improved measurements of shear modulus and pleural membrane tension of the lung. J. Appl. Physiol. 47, 175-181.

He, L., Lim, C., Wu, B., 2004. A continuum model for size-dependent deformation of elastic films of nano-scale thickness. Int. J. Solids Struct. 41, 847–857.

Huang, D., 2008. Size-dependent response of ultra-thin films with surface effects. Int. J. Solids Struct. 45, 568–579.

Hui, C.Y., Liu, T.S., Salez, T., Raphael, E., Jagota, A., 2015. Indentation of a rigid sphere into an elastic substrate with surface tension and adhesion. Proc. R. Soc. A 471, 20140727.

Johnson, K.L., Kendall, K., Roberts, A.D., 1971. Surface energy and the contact of elastic solids. Proc. R. Soc. Lond. A 324, 301–313.

Lu, C., Wu, D., Chen, W., 2011. Nonlinear responses of nanoscale FGM films including the effects of surface energies. IEEE T Nanotechnol. 10, 1321–1327.

Maugis, D., 1992. Adhesion of spheres: The JKR–DMT transition using a Dugdale model. J. Colloid Interface Sci.150, 243–269.

Miller, R.E., Shenoy, V.B., 2000. Size-dependent elastic properties of nanosized structural elements. Nanotechnology. 11, 139–147.

Mogilevskaya, S.G., Pyatigorets, A.V., Crouch, S.L., 2011. Green function for the problem of a plane containing a circular hole with surface effects. J. Appl. Mech. 78, 021008.

Orsello, C. E., Lauffenburger, D. A., Hammer, D. A., 2001. Molecular properties in cell adhesion: a physical and engineering perspective. Trends Biotechnol, 19, 310–316.

Qian, J., Wang, J.Z., Gao, H., 2008. Lifetime and strength of adhesive molecular bond clusters

between elastic media. Langmuir 24, 1262–1270.

Qian, J., Wang, J.Z., Lin, Y., Gao, H., 2009. Lifetime and strength of periodic bond clusters between elastic media under inclined loading. Biophys. J. 97, 2438–2445.

Qian, J., Lin, Y., Jiang, H.Y., Yao, H.M., 2013. Bond formation of surface-tethered receptor-ligand pairs in relative separation. Appl. Phys. Lett. 103, 223702.

Qian, J., Lin, J., Xu, G-K., Lin, Y., Gao, H., 2017. Thermally assisted peeling of an elastic strip in adhesion with a substrate via molecular bonds. J. Mech. Phys. Solids 101, 197–208.

Shenoy, V.B., 2002. Size-dependent rigidities of nanosized torsional elements. Int. J. Solids Struct. 39, 4039–4052.

Wang, J.Z., Gao, H., 2010. Size and shape dependent steady-state pull-off force in molecular adhesion between soft elastic materials. Int J. Fract 166, 13–19.

Wang, J., Qian, J., Gao, H., 2008. Stability of molecular adhesion mediated by confined polymer repellers and ligand-receptor bonds. Mol. Cell. Biol. 5, 19–25.

Zhu, X.Y., Xu W., 2018. Effect of surface tension on the behavior of adhesive contact based on Lennard-Jones potential law. J. Mech. Phys. Solids. 111, 170–183.